**International Journal of Power Electronics and Drive System (IJPEDS)**
Vol. 8, No. 2, June 2017, pp. 812~825
ISSN: 2088-8694, DOI: 10.11591/ijpeds.v8i2.pp812-825


# ZVS Full Bridge Series Resonant Boost Converter with Series-Connected Transformer

**Mohamed Salem[1], Awang Jusoh[2], N. Rumzi N. Idris[3], Tole Sutikno[4], Iftikhar Abid[5]**
[1, 2, 3]Faculty of Electrical Engineering, Universiti Teknologi Malaysia, 81300 Skudai, Malaysia.
[4]Department of Electrical Engineering, Universitas Ahmad Dahlan, Indonesia.
[5]Advanced Photon Source, Argonne National Laboratory, Cass Avenue, Argonne, USA

**Article Info**

***Article history:***

Received Feb 3, 2017
Revised Apr 3, 2017
Accepted Apr 17, 2017

***Keyword:***

Full bridge converter
High frequency transformer
Series resonant converter
Soft switching
Zero voltage switching

**ABSTRACT**

This paper presents a study on a new full bridge series resonant converter (SRC) with wide zero voltage switching (ZVS) range, and higher output voltage. The high frequency transformer is connected in series with the LC series resonant tank. The tank inductance is therefore increased; all switches having the ability to turn on at ZVS, with lower switching frequency than the LC tank resonant frequency. Moreover, the step-up high frequency (HF) transformer design steps are introduced in order to increase the output voltage to overcome the gain limitation of the conventional SRC. Compared to the conventional SRC, the proposed converter has higher energy conversion, able to increase the ZVS range by 36%, and provide much higher output power. Finally, the a laboratory prototypes of the both converters with the same resonant tank parameters and input voltage are examined based on 1 and 2.2 kW power resprctively, for veryfing the reliability of the performance and the operation principles of both converters.



***Corresponding Author:***

Mohamed Salem,
Energy Conversion Engineering Department,
Faculty of Electrical Engineering,
Universiti Teknologi Malaysia,
81300 Skudai, Malaysia.
Email: moha_so_2009@yahoo.com / smohamed3@live.utm.my

## 1. INTRODUCTION

Resonant converters have been extensively studied since the 80s [1]. They provide the possibility to achieve low switching losses and allow switches to control resonance at high switching frequency. However, increasing the operating frequency will increase the switching losses and decrease the system efficiency. An answer to this problem is to replace the "Chopper" switch of a standard topology by a "resonant" switch, which uses the resonances of circuit capacitances and inductances to shape the waveform, which then shapes the current or voltage through the switching element. Therefore, when switching takes place, there is no current or the voltage flowing through it. A zero current switching (ZCS) characterizes the current waveform, while a zero voltage switching circuit (ZVS) characterizes the voltage waveform. The resonant converter not only achieves soft switching at turn on and off, but also has less switching losses compared to PWM hard switching converter. For resonant converter, the soft switching method depends on the ratio of the normalized frequency. If the normalized frequency F is higher than unity (1), the performance of the converter will be under ZVS condition. Meanwhile, if it is less than unity, the performance of the converter will be under ZCS condition [2]. Furthermore, a high switching frequency is required in such converters to cut down the size and weight of the converter. At high frequencies, the converter has the ability to achieve soft-switching which is used to reduce the switching losses. However, this will cause high electromagnetic interference di/dt and dv/dt, which still can affect the system efficiency [3]-[7]. Series resonant converter

(SRC) has been recommended by many researchers in many applications due to its simplicity and popularity [8]-[10] since the LC components are connected in series with the rectifier-load network. The drawback of SRCs is that the input voltage is split between resonant impedance and load, which makes the DC gain of SRC always lower than unity [11]-[12]. In case of light load or no-load condition, it is difficult to control the output voltage. Thus, ZVS is limited to a specific load conditions and input voltage ranges [13]. Several schemes have been developed to solve these problems, such as LLC series resonant converter topologies, which have gained many attention due to their merit of efficient conversion and high voltage gain [14]-[16]. These topologies have been introduced with full or half bridge inverters and either center tapped or full bridge rectifiers, the center tapped rectifier however is not preferred due the high voltage stress on the diodes [17]-[20]. The LLC output voltage or current can be regulated in a wide range by varying the switching frequency [21]-[23]. Medium and high voltage converters with full and half- bridge have been presented and developed in many industry applications. Majority of previous works have covered the half bridge for a resonant converter and have been presented in multilevel inverters with interleaved resonant tank, due to the fact that full bridge converters cause high circulating current losses and narrow range of ZVS [20, 24-26].

This paper presents the design consideration of full bridge series resonant converter that capable of working above resonant frequency to achieve ZVS turn-on for all power switches. The converter has been tested with different values of switching frequency in order to investigate the operation region of ZVS and to clarify the boundary between ZVS and ZCS. Furthermore, a high frequency step-up transformer has been designed and connected in series with proposed resonant tank and the full bridge rectifier in order to function as the following: (1) turn on ZVS for all switches; (2) to compare wide ZVS range with respect to the conventional series resonant converter; (3) to decrease the switching frequency to reduce the electromagnetic interference; (4) to produce high conversion efficiency and high power density; and (5) to reduce voltage stress of power switches. Finally, to corroborate the validity and analysis of wide range of turned-on zero voltage switching of the series resonant DC DC converter, an experiment of the proposed converter based on a 2.2 kW laboratory prototype has been conducted.

## 2. FULL-BRIDGE SERIES RESONANT CONVERTER (SRC

The basic components of the SRC are shown in Figure 1. Each part of the converter performs a specific task, as summarized in this section. The DC source powers the full bridge inverter switches which rapidly turns on and off, according to the switching frequency, to generate the output voltage, and average value of the switched-input voltage during the specific time period. To reduce electromagnetic interference and harmonic distortion, a resonant tank containing L and C is used to generate sinusoidal voltage and current signals [27]. Since this RC tank component is used as an energy buffer between the the switching network and the rectifier network, the tank values can be determined by the frequency selective network. The principle is that, under resonance condition, the impedance of inductance must be equal to the capacitance, thus generates the resonance frequency. Ultimately, the output signal is rectified and filtered to generate the desired DC output voltage [28]. Once the resonant tank impedance value is chosen, the tank current should be ensured enough to reach the output. From the tank parameters, resonant frequency and the tank impedance equations can be obtained as in equation (2) and (3):

$$f_s = \frac{1}{T_s} \tag{1}$$

$$f_0 = \frac{1}{2\pi\sqrt{LC}} \tag{2}$$

$$Z_0 = \sqrt{\frac{L}{C}} \tag{3}$$

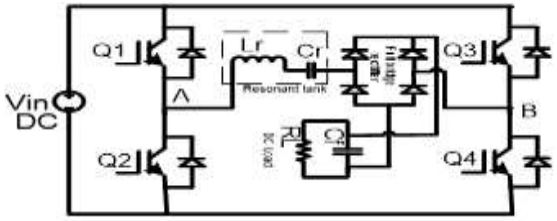


Figure 1. The typical configuration of the (SRC)

### 2.1. Series Resonant Converter Characteristics

In SRC, the tank is linked in series with the rectifier-load network. The load and resonant tank function as a voltage divider. The impedance of resonant tank will be changed by altering the frequency of driving voltage to the resonant network, which as depicted in Figure 2. The input voltage is split between this impedance and the effective resistance [11]. The DC gain of SRC is always lower than unity, because it works as a voltage divider. The gain can be calculated by using the gain equation M, Equation 4. At light-load condition, if the load resistance is too large compared to the impedance of the resonant network Z0, all the input voltages will be imposed on the load. This makes it difficult to modulate the output at light load.

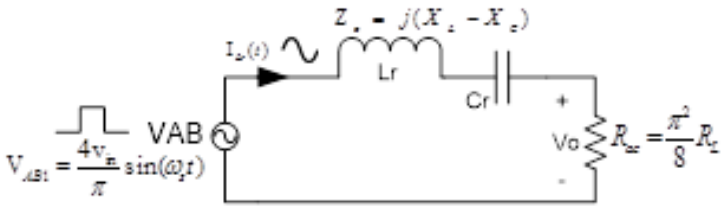


Figure 2. Equivalent circuit of the dc-dc series resonant converter

$$M = \frac{V_o}{V_{in}} = \frac{1}{\sqrt{1+\frac{(\pi Q)^2}{8}(\frac{1}{F}-F)^2}} \quad (4)$$

The modes of operations of the SRC can be divided into three categories based on switching frequency, conduction mode, and proficiency of the soft switching. Consequently, for the load parameters and command for the ranges, the SRC has an uncountable number of modes of operations. These modes and the boundaries between each of them have been explained and studied in detail in [29]. The conduction modes are grouped into two areas of discontinuous conduction mode (DCM) and two ranges of the continuous conduction mode (CCM and CCM1) based on the normalized frequency as summarized in Table 1. In summary, in order to design converter to work under ZVS, the resonant thank should be an inductive response, which means that, the switching frequency should be above the tank frequency [30].

Table 1. Summary of Series resonant converter modes

| Conduction mode | Frequency range | Switch transition | ZCS | ZVS |
|---|---|---|---|---|
| DCM | $0 \le F \ge 0.5$ | Turn-on | yes | no |
| | | Turn-off | yes | yes |
| CCM | $0.5 \le F \ge 1$ | Turn-on | no | no |
| | | Turn-off | yes | yes |
| CCM1 | $F \ge 1$ | Turn-on | yes | yes |
| | | Turn-off | no | no |

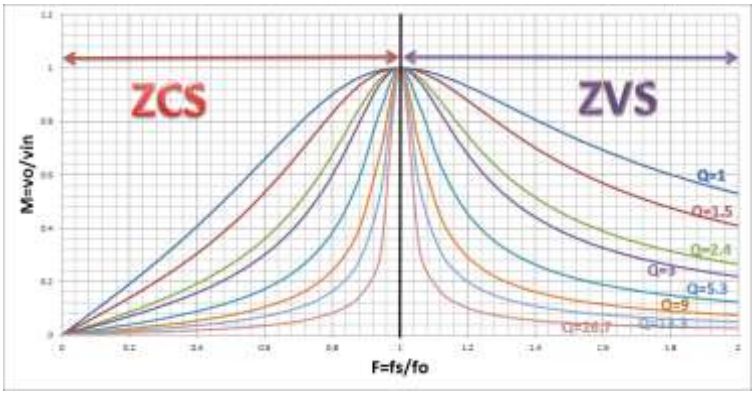


Figure 3. The gain characteristics of the SRC, for the range 0 ≤ F ≥ 2

The gain curves and the soft switching boundaries are shown in Figure 3. It can be seen that, in case of operating above resonance, increasing the switching frequency will cause reduction in output voltage. The output voltage can be increased by decreasing the Q, which will increase the load resistance. At low value of Q less than 0.785, the converter will gain unity before resonant frequency. Therefore, the converter will begin to operate under DCM, while maintaining the output potential of the same value at each frequency. To avoid this problem, the Q value should be sufficient to hold the high output voltage by small alterations in the frequency and to utilize zero-voltage switching.

### 2.2. Operating Above Resonance

Under steady state, the full bridge SRC switching above resonant has four operating modes. In one complete cycle, each mode is taken and explained individually in this section. The initial values of each mode can be calculated at the last point from the previous mode. The voltage and current waveforms of the operation modes are plotted in Figure 4.

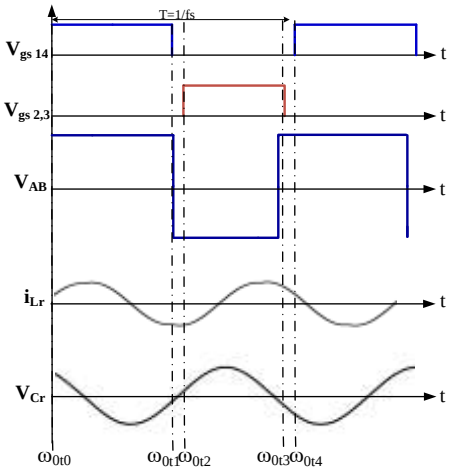


Figure 4. Operational waveforms of full-bridge (SRC) working above resonant

#### 2.2.1. Mode I: (between $\omega_0 t_0$ and $\omega_0 t_1$)

When the freewheeling diodes of the switches Q1 and Q4 are turned on, part of the tank energy feeds the load and the rest is delivered back to the source; thus resonant current ilr dies down at ω0t0, and starts to reverse. Because the current changes its track from freewheeling diodes to the power switches Q1 and Q4, in this mode, the switches are turned on at zero voltage switching. The instantaneous resonant voltage and current can be evaluated by using:

$$I_{Lr}(t) = \frac{1}{Z_o}[V_{in} - V_o - V_{cr}(0)] sin\ \omega_0 t \quad (5)$$

$$V_{cr}(t) = V_{in} - U_0 - [V_{in} - V_0 - V_{cr}(0)] cos\omega_0 t \quad (6)$$

#### 2.2.2. Mode II: (between $\omega_0 t_1$ and $\omega_0 t_2$)

When the resonant capacitor voltage $V_{cr}$ crosses zero at the instant $\omega_0 t_1$, switches $Q_1$ and $Q_4$ are forced to turn off. Turn off losses exist because they are hard switching, but they can be eliminated by using small capacitors across the switches. The current starts to flow through the freewheeling diodes of the switches $Q_2$ and $Q_3$, and results in the power stage, which means that, the source feeds the tank, so the negative voltage across the tank forces the current to drop to zero at end of this mode. The voltage and current for this mode are given by the following equations:

$$I_{Lr}(t) = \frac{1}{Z_o}[-V_{in} - V_o - V_{cr}(1)] sin\ \omega_0(t - t_0) + I_{Lr}(1) cos\ \omega_0(t - t_0) \quad (7)$$

$$V_{cr}(t) = V_{cr}(1) + \frac{I_{Lr}(1)}{\omega_0} sin\ \omega_0(t - t_0) + [-V_{in} - V_0 - V_{cr}(1)][1 - cos\ \omega_0(t - t_0)] \quad (8)$$

**2.2.3. Mode III: (between $\omega_0 t_2$ and $\omega_0 t_3$)**

The diodes of switches $Q_2$ and $Q_3$, will be opened circuit at beginning of this mode at $\omega_0 t_2$, and the resonant stage between the tank components will be achieved. As the current flows through the freewheeling diodes, switches $Q_2$ and $Q_3$ are turned on under zero voltage switching conditions. During this interval, the tank energy is imposed to the load, so the polarity of the output voltage seen by the tank changes with the resonant current. Meanwhile, the resonant capacitor voltage is shifted with respect of the current, where, it is at peak when the current is zero and clamped to zero expressed as follows:

$$I_{Lr}(t) = \frac{1}{Z_o}[-V_{in} + V_o - V_{cr}(2)]sin\ \omega_0(t - t_2) \quad (9)$$

$$V_{cr}(t) = -V_{in} + V_0\text{-}[-V_{in} + V_0 - V_{cr}(2)]cos\ \omega_0(t - t_2) \quad (10)$$

**2.2.4. Mode IV: (between $\omega_0 t_3$ and $\omega_0 t_4$)**

In this interval, the hard switching turn off is occured for the switches $Q_2$ and $Q_3$ at $\omega_0 t_3$. Therefore, the current naturally will change its track to the freewheeling diodes of switches $Q_1$ and $Q_4$, and the resonant current will reach zero at $\omega_0 t_4$, which means, the first switching period ends, and the operation to the first mode is in the following subsequent cycle. The instantaneous resonant voltage and current for this mode can be estimated by using:

$$I_{Lr}(t) = \frac{1}{Z_o}[V_{in} + V_o - V_{cr}(3)]sin\ \omega_0(t - t_3)\ + I_{Lr}(3)cos\ \omega_0(t - t_3) \quad (11)$$

$$U_{cr}(t) = V_{in} + V_0 + I_{Lr}(3)Z_o sin\ \omega_0(t - t_3)\ \text{-}[V_{in} + V_0 - V_{cr}(3)]cos\ \omega_0(t - t_3) \quad (12)$$

## 3. SERIES RESONANT CONVERTER WITH SERIES CONNECTED TRANSFORMER (LLC)

The concept of this converter does not have many difference compared to the converter as mentioned in the previous section. It can be considered as an improvement topology of the previous one as it eliminates some of the weaknesses of the SRCs, such as the limitation of the output voltage, and the limited switching frequency to achieve the ZVS. The SRC gain is always less than unity. The aim of this method is to use a step up high high frequency transformer connected in series with the LC tank, as illustrated in Figure 5. This to meet the requirements of the converter to increase the output power and enhance the resonant inductance by the magnetizing inductee of the transformer, where, it will be involved in the resonant tank and will lead to increase in the zero voltage switching range.

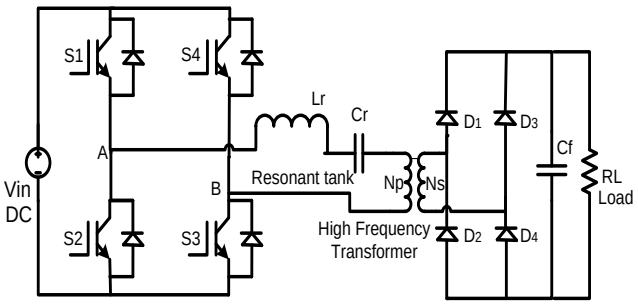


Figure 5. The configuration of the (SRC) with series connected transformer

### 3.1. HF Transformer Design

In order to compare these converters and to prove the extension of the zero voltage switching range, the HF transformer must be designed to work at lower frequency than the resonant frequency. Moreover, for practical design, many requirements must be taken into account. For example, the primary winding of the transformer are connected in series with the resonant tank, so they have the same value of the current. The output voltage also equal to the secondary voltage of the HF transformer, so the primary voltage is the winding ratio to the output voltage. For this work, the primary voltage is the output voltage of the LC

resonant tank. The operating frequency is 37.5 kHz and the selected transformer core is ETD 39. The maximum flux destiny (Bm) must be considered carefully to avoid saturation and under utilizing the core situations. Therefore, the maximum flux density must be in the range of 1300G to 2000G, which is acceptable for most transformer cores. Based on these design considerations, the number of required primary and secondary turns can be obtained by assuming the value of the flux destiny as in the following expression:

$$N_{Pri} = \frac{U_{Pri(nom)}10^8}{4\,f_s B_m A_c} = \frac{20*10^8}{4\,f_s 1500*1.25} = 7\ turns \quad (13)$$

$$N = 7 = \frac{U_O}{U_{Pri}} = \frac{N_{sec}}{N_{Pri}},\ N_{sec} = 49\ turns \quad (14)$$

### 3.2. Operating Principle

The topology of the SRC with series connected transformer schematic consists three main stages, as shown in Figure 5.

#### 3.2.1. Control Switching Network (CSN)

In this stage, the switching network is represented in a full bridge inverter. The switches of the CSN work alternately, to produce a square wave of voltage $V_{AB}(t)$ which is expressed by Fourier series in (15), to feed the resonant thank. Meanwhile, $Q_1$ and $Q_3$ are triggered simultaneously by 50% duty cycle for the first half cycle, then the other two switches, which are $Q_2$, $Q_4$, are trigged for the second half cycle. Small dead time must be introduced to avoid the signals interfaces and to allow the soft switching to occur.

$$U_{AB}(t) = \frac{4V_{in}}{\pi}\sum\frac{1}{n}\sin(n\omega_s t) \quad where\ n = 1,3,5\ \ldots. \quad (15)$$

#### 3.2.2. Resonant Tank Network (RTN)

In this topology, the resonant tank consists of resonant inductive $L_r$, resonant capacitor $C_r$ and the magnetizing inductance of the step up transformer, as shown in Figure 6. The tank allows only the sinusoidal current to follow through the RTN. Moreover, the resonant current or the primary current lags the square voltage that is applied to the RTN, as long the converter works under an inductive mode, to achieve the ZVS turns on for the switches.

#### 3.2.3 Diode Rectifier Network with Low Pass Filter (DR_LPF)

The full bridge diode network is used to rectify the AC variables to produce the desired DC output voltage, and the filtering process of the resonant tank allows the use of the fundamental approximation to obtain the gain of the topology. Figure 6 describes the relation between the equivalent load resistance and the actual load resistance, and the average of the current Iac is equal to the output current $I_o$. The harmonic components of the resonant tank output voltage $V_R(t)$ are not involved in the power transfer. Also, with considering the transformer turns ratio, the equivalent load resistance related to the primary side is obtained, as shown in Figure 6b.

$$U_R(t) = \frac{4V_o}{\pi}\sum\frac{1}{n}\sin(n\omega_s t) \quad where\ n = 1,3,5\ \ldots. \quad (16)$$

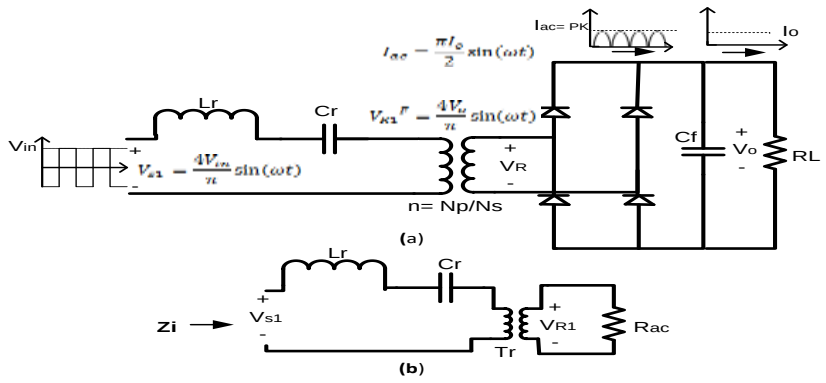


Figure 6. a) The stages and the variables of the converter topology. b) AC equivalent circuit with series connected transformer

### 3.3. Circuit Characteristics

The voltage gain M of this topology can be classified into three stages: the gain of the switched full-bridge, the gain of the resonant tank and the transformer turns ratio. The gain of the switched full-bridge and the transformer turns are fixed components, while the resonant tank is variable gain. Based on Figure 6-b, the voltage gain characteristics of tank can be represented as a function of normalized frequency ratio ($F=f_s/f_{r1}$), load quality factor (Q) and factor of related total primary inductance to the resonance inductance ($A_L$), which is considered as a fixed parameter as it is does not change with the operation. Consequently, this tank has two resonant frequencies: the higher resonant frequency, $f_{r1}$ which is caused by the resonant elements $L_r$ and $C_r$, while the $f_{r2}$ is obtained by all the tank parameters as defined in Equation (19). In practice, the voltage gain can be determined by:

$$M = \frac{V_o}{V_{in}} = \frac{F^2(A_L-1)}{\sqrt{(\frac{f_s{}^2}{f^2{}_{r2}}-1)^2+(Q(F^3-F)^2(A_L-1))^2}}\ 1.25 \quad (17)$$

$$A_L = 2.5 = \frac{L_r+L_m}{L_r}\ , L_m = 300\ \mu H \quad (18)$$

$$f_{r1} = \frac{1}{2\pi\sqrt{L_r c_r}} = 42.5\ kHz\ , f_{r2} == 26.9\ kHz \quad (19)$$

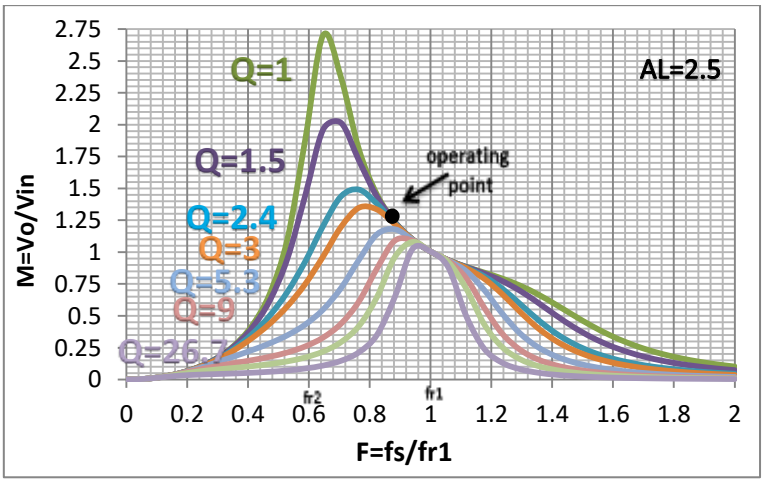


Figure 7. The gain characteristics of the SRC with the series step up HF, for the range $0 \leq F \geq 2$, and different load factor

As one can observe from the gain curves for different Q values, i) in case of operation above resonance ($f_s>fr_1$), the converter seems to behave as the conventional series resonant converter. Since the gain is less than unity for the entire region, and it decreased as the operating frequency gets apart from resonant frequency. Therefore, this region is defined as an inductive region, and only ZVS will be achieved. Meanwhile, ii) in case of operation at resonance ($f_s=fr_1$), it is obvious from Figure 7, that the gain is unity for the all Q values, which means, operating at resonant frequency is not effect by load variation and the output voltage will remain the same with the input voltage. Furthermore, operation below resonance can be divided into two regions: iii-a) the region between resonant frequencies ($fr_2<f_s>fr_1$), where, in this region, the gain is higher than 1and the peak gain depends on the Q value. Meanwhile, for low Q values (light loads), the gain could reach the maximum point where we can obtain the minimum load factor Qmin. Unlike, for high Q values (heavy loads) where we are able to obtain the maximum load factor Qmax. Based on our design parameters at switching frequency of 37.5 kHz and AL=3, the load factor is in range of (1-3), in order to achieve the maximum voltage gain equal to 1.25. iii-b) for the region with switching frequency lower than second resonant frequency ($f_s<fr_2$). The gain for all Q values starts to drop to zero as soon as the switching frequency decreases. Moreover, in this region, the period of switching frequency is much lower than resonant period. Therefore, the resonant cycle is not able to finish for this reason the discontinuous mode will be carried out.

## 4. EXPERIMENTAL RESULTS

In this study, two experimental prototypes of the conventional SRC and the proposed converter had been tested to verify the performance and the extended range of ZVS. The first circuit was tested and imposed with different switching frequencies to investigate the ZVS range. Meanwhile, the proposed converter was tested by using the same parameters and switching frequency that was lower than resonant frequency in order to certify the theoretical parts as derived in the previous section. The converters were implemented with the following specifications: $V_{in}$=180 V, resonant capacitor=70 nF with resonant frequency= 42.5 kHz, output capacitor Cf=4 uf, and the selected load factor Q=2.4. Power switch IGBTs TQ-247AC was selected based on their advantages of fast switching and application capability. The circuit shown in Figure 1 was tested and imposed with different switching frequencies to investigate the reliability of the ZVS range. Microcontroller eZdspTM F28335 was used to implement the gate pulses from software to gate drives. The gate signals had been validated with 50 kHz switching frequency before being sent to the switches as shown in Figure 8. Signals 1 and 3 worked simultaneously for the first half cycle. Then, the other two signals, 2 and 4 worked for the second half of switching cycle. A dead time was ensured with a value of 0.5µs, to avoid the signals interface and to offer a matter of time to allow ZVS to occur.

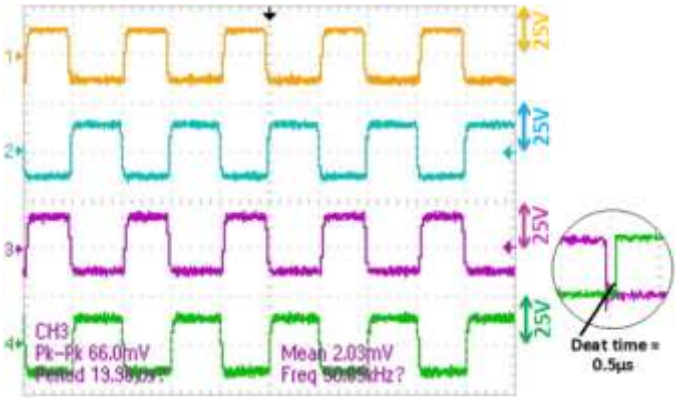


Figure 8. Gate driver signals at 50 kHz switching frequency

Figure 9 shows the LC tank waveforms. The full bridge switching generates square wave voltage VAB that excited the resonant tank and created the sinusoidal wave forms. It was obvious that the resonant current started by a negative polarity at each half cycle, which allowed the ZVS to be achieved for the switching frequency higher than resonant frequency. Meanwhile, at lower switching frequency the ZCS was achieved. At fs=37.5 kHz, the switching period was much lower than resonant period. Therefore, the resonant waveforms were not able to finish their cycle, due to the DCM condition.

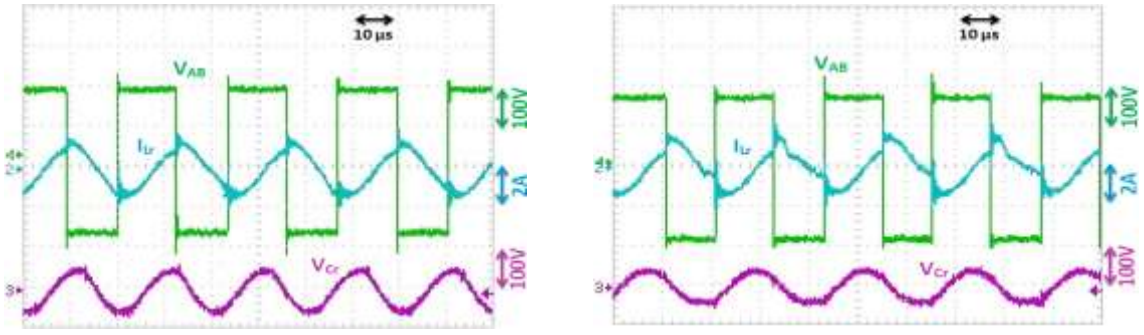


(a) (b)

Figure 9. Measured waveformes of the resonant tank input voltage VAB, resonant inductor current iLr and resonant capacitor voltage Vcr of conventional SRC at Vin=180 and (a) $f_s$=50 kHz, (b) $f_s$=45 kHz

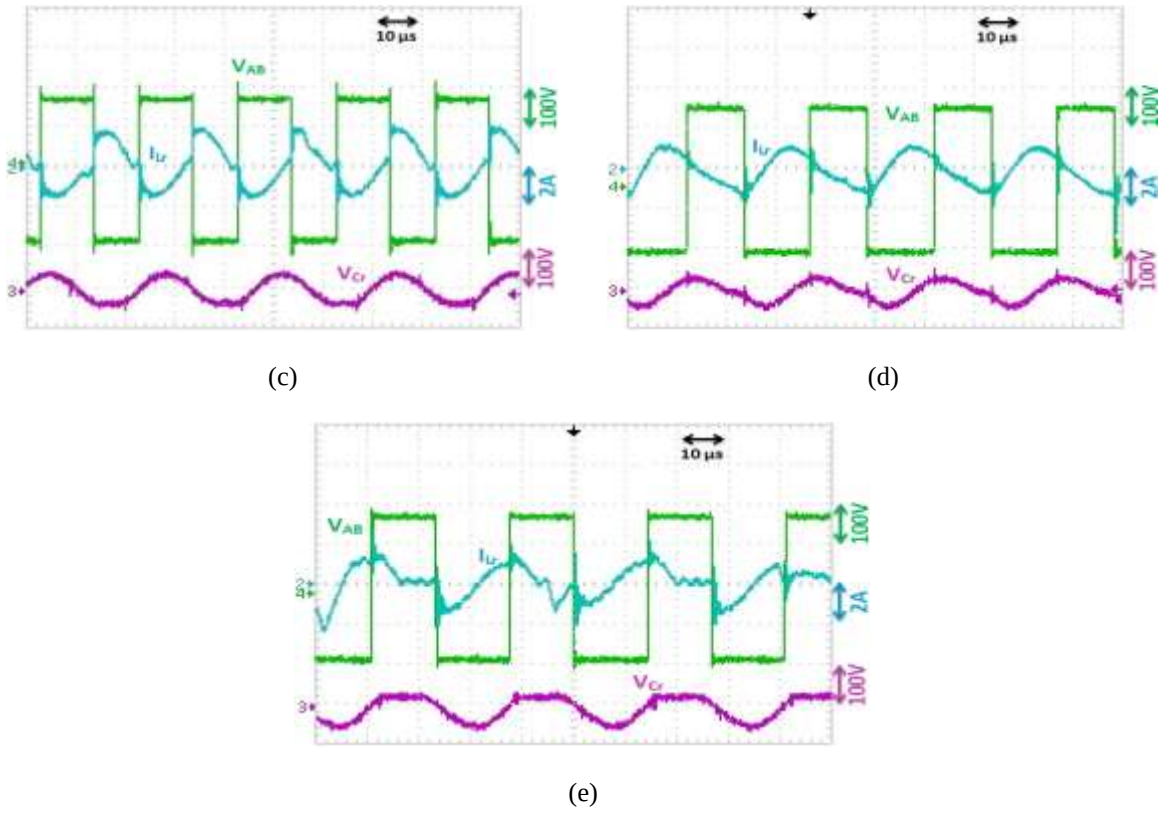


Figure 9. Measured waveformes of the resonant tank input voltage VAB, resonant inductor current iLr and resonant capacitor voltage Vcr of conventional SRC at Vin=180 and (c) $f_s$=42.5kHz, (d) $f_s$=40 kHz, and (e) $f_s$=37.5 kHz.

Figure 10 shows the gate voltage and collector voltage of all switches at 50 kHz, 45 kHz, and 42.5 kHz switching frequency conditions. The collector voltage $V_{CE}$ dropped to zero, before the switches were turned on. Thus, all the switches were turned on at ZVS, similar at 40 kHz, and 37.5 kHz conditions. The switches were turned off before the collector voltage was risen to the input voltage value. Therefore, all the switches were turned off at ZCS.

The experimental results based on the SRC with series connected transformer with the same circuit parameters of the conventional SRC was provided to verify the theoretical and the design parts. The measured waveforms of the resonant tank which were; the tank input voltage $V_{AB}$, the resonant inductor current (the primary side current), and the resonant capacitor voltage, are shown in Figure 11(a). Meanwhile, the secondary voltage and current are illustrated in Figure 11(b). It was obvious that, the primary side had the same shapes of the conventional SRC with small changes in the resonant current and voltage values, and more stress was noticed especially in the secondary waveforms, because of the magnetizing inductance of the transformer. Moreover, compared this prototype to the conventional SRC under the same switching frequency, it is clear that the proposed converter can provide more energy conversion and higher output voltage than the input, and it works under CCM. Figure 12 shows the prove of the possibility of increasing the ZVS range, where all the switches were turned on at ZVS. Therefore, the SRC with series connected transformer seems provide a better choice as it can solve some of the conventional SRC weaknesses.

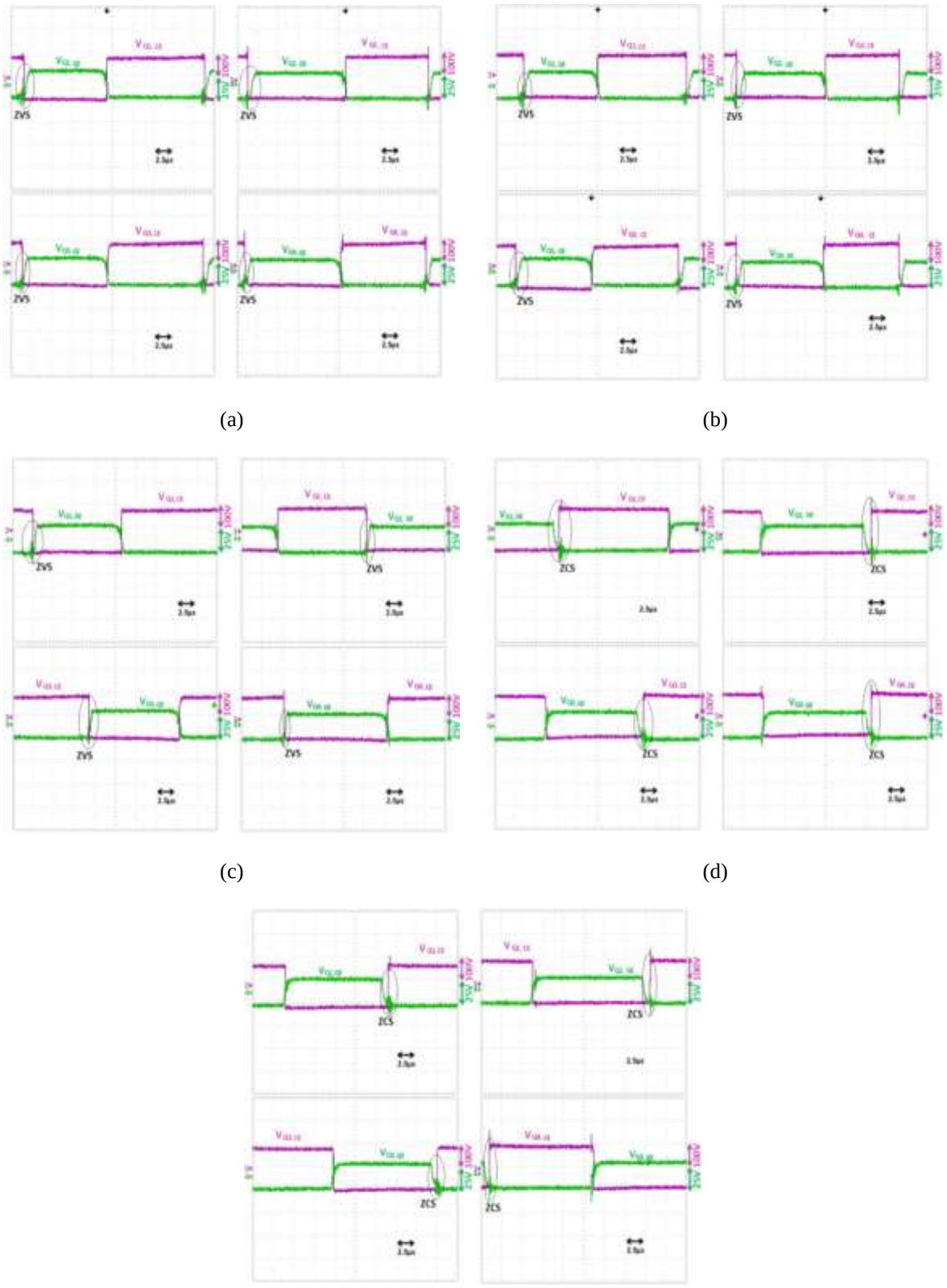


(a) (b)

(c) (d)

(e)

Figure 10. Measured waveformes of the gate voltage and collector voltage of all switches at Vin=180 V and (a)fs=50 kHz, (b) fs=45 kHz, (c) fs=42.5 kHz, (d) fs=40 kHz ,and (e) fs=37.5 kHz .

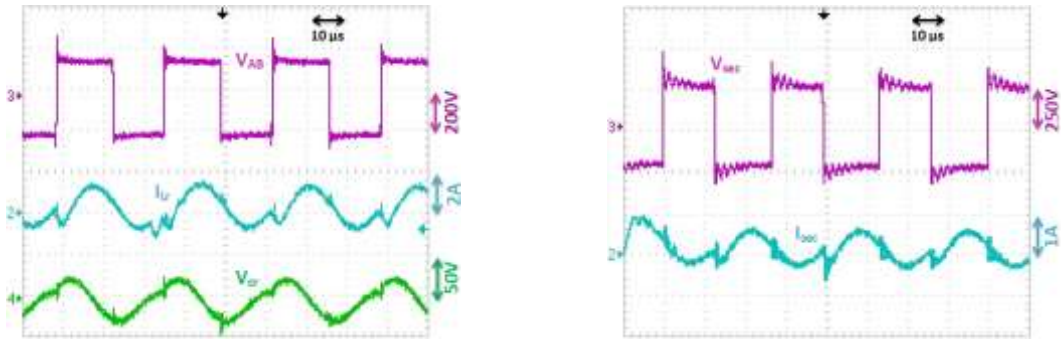


Figure 11. Measured results of the SRC with series connected transformer with Vin=180, fs=37.5 kHz and Q=2.4 (a) resonant tank waveforms; resonant tank input voltage $V_{AB}$, resonant inductor current $i_{Lr}$ and resonant capacitor voltage $V_{cr}$. (b) the secondary side voltage and current waveforms.

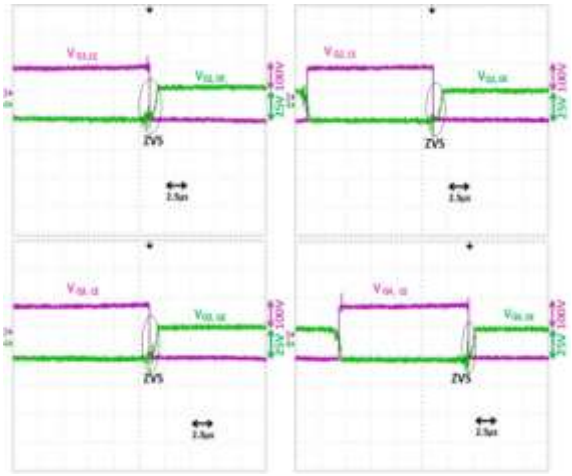


Figure 12. Measured waveformes of the gate voltage and collector voltage of all switches of the SRC with series connected transformer at Vin=180 V and fs=37.5kHz

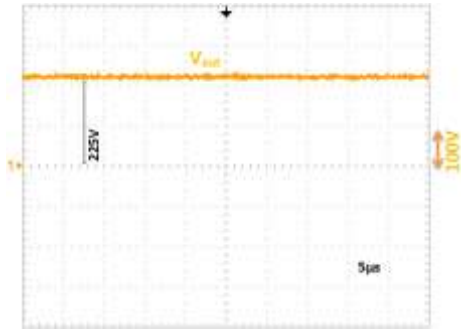


Figure 13. Measured waveform of the output

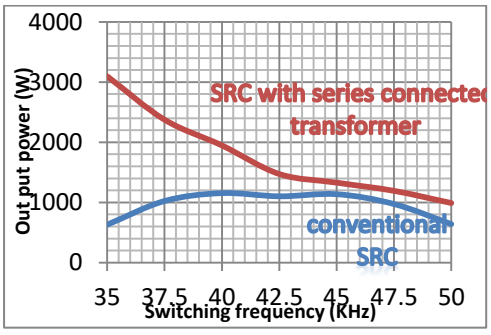


Figure 14. Measured converte output power at different switching frequencies

The rectified output voltage is given in the plot of Figure 13. The magnitude of output voltage was higher than the input, as explained in theoretical part. The SRC with step-up transformer was able to overcome the gain limitation. The voltage could reach to 1.25 times of the input voltage with lower switching frequency and load factor less than 1. The output power with different switching frequencies for both converters are shown in Figure 14. The maximum ouput power was obtained when the switching frequency was close to the resonant frequency, and decreased as the switching frequency became much higher or lower

than resonant frequency. Meanwhile, for the SRC with series step-up connected transformer, the output power was higher than the conventional under all switching frequencies and it increased as the switching frequency decreased.

## 5. CONCLUSION

For conventional SRC, the ZVS turn on for all switches can be only achieved if the switching frequency is higher than resonant frequency, in which the gain is lower than unity. The performance of the SRC with series connected transformer has been compared to the conventional SRC under the same tank parameters and input voltage. The HF step-up transformer has been designed to enhance the resonant tank inductivity and to increase the output voltage. The ZVS range has been successfully extended by 36%, tested and proven its reliability with switching frequency of 37.5 kHz which means extended by 12% ( extended from 42.5 kHz to 37.5 kHz) compared to the conventional SRC. Moreover, the energy transferred from the input to the output has been significantly increased. On top of that, the output voltage is 25% higher than the input voltage. Meanwhile, the current and voltage stress are slightly higher because of minimizing the switching frequency. Based on these improvements, the series resonant converter with transformer can provide much better results and eliminate the limitations of the conventional SRC. Finally in order to verify the reliability of the performance and the operation principles of the proposed converter, the experiment prototypes of the conventional and the proposed SRC are provided with power rating of 1000 W and 2200 W respectively.

## REFERENCES


[1] R. Severns, "Topologies for three element resonant converters," *in Applied Power Electronics Conference and Exposition, 1990. APEC'90, Conference Proceedings 1990, Fifth Annual*, pp. 712-722, 1990.

[2] K.-H. Liu, R. Oruganti, and F. C. Lee, "Resonant switches-Topologies and characteristics," *in Power Electronics Specialists Conference, 1985 IEEE*, 1985, pp. 106-116, 1985.

[3] J. Javidan, "Design of a ZVS PWM DC–DC converter for high gain applications," *International Journal of Circuit Theory and Application*s, 2015.

[4] M. Salem, A. Jusoh, N. R. N. Idris, and I. Alhamrouni, "Performance study of series resonant converter using zero voltage switching," *in Energy Conversion (CENCON), 2014 IEEE Conference* on, pp. 96-100, 2014.

[5] K. D. Ngo, "Analysis of a series resonant converter pulse width-modulated or current-controlled for low switching loss," *IEEE transactions on power electronics*, vol. 3, pp. 55-63, 1988.

[6] M. Salem, A. Jusoh, N. R. N. Idris, and I. Alhamrouni, "Modeling and simulation of generalized state space averaging for series resonant converter," *in Power Engineering Conference (AUPEC), 2014 Australasian Universities*, pp. 1-5, 2014.

[7] M. T. Outeiro and G. Buja, "Comparison of resonant power converters with two, three, and four energy storage elements," *in Industrial Electronics Society, IECON 2015-41st Annual Conference of the IEEE, pp. 001406-001411, 2015.*

[8] H. Chan, K. Cheng, and D. Sutanto, "Phase-shift controlled DC-DC convertor with bi-directional power flow," *IEE Proceedings-Electric Power Applications*, vol. 148, pp. 193-201, 2001.

[9] C.-H. Chien, Y.-H. Wang, and B.-R. Lin, "Series Resonant Converter with Series-Parallel transformers for high input voltage applications," *in TENCON 2011-2011 IEEE Region 10 Conference*, pp. 873-877, 2011.

[10] X. Xie, J. Zhang, C. Zhao, Z. Zhao, and Z. Qian, "Analysis and optimization of LLC resonant converter with a novel over-current protection circuit," *IEEE Transactions on Power Electronics*, vol. 22, pp. 435-443, 2007.

[11] R. L. Steigerwald, "A comparison of half-bridge resonant converter topologies," *IEEE Transactions on power electronics*, vol. 3, pp. 174-182, 1988.

[12] R. W. Erickson and D. Maksimovic, Fundamentals of power electronics: Springer Science & Business Media, 2007.

[13] B.-R. Lin and S.-F. Wu, "ZVS resonant converter with series-connected transformers," *IEEE Transactions on Industrial Electronics*, vol. 58, pp. 3547-3554, 2011.

[14] J. Ke and R. Xinbo, "Hybrid full bridge three-level LLC resonant converter," *Proceedings of the CSEE*, vol. 26, pp. 53-58, 2006.

[15] S. De Simone, C. Adragna, and C. Spini, "Design guideline for magnetic integration in LLC resonant converters," *in Power Electronics, Electrical Drives, Automation and Motion, 2008. SPEEDAM 2008. International Symposium on, pp. 950-957, 2008.*

[16] F. Musavi, M. Craciun, D. S. Gautam, and W. Eberle, "Control strategies for wide output voltage range LLC resonant DC–DC converters in battery chargers," *IEEE Transactions on Vehicular Technology*, vol. 63, pp. 1117-1125, 2014.

[17] G. Ivensky, S. Bronshtein, and A. Abramovitz, "Approximate analysis of resonant LLC DC-DC converter," *IEEE Transactions on power electronics*, vol. 26, pp. 3274-3284, 2011.

[18] M. K. Kazimierczuk and D. Czarkowski, Resonant power converters: John Wiley & Sons, 2012.

[19] J. Deng, S. Li, S. Hu, C. C. Mi, and R. Ma, "Design methodology of LLC resonant converters for electric vehicle battery chargers," *IEEE Transactions on Vehicular Technology*, vol. 63, pp. 1581-1592, 2014.

[20] B.-R. Lin and C.-H. Liu, "Analysis, design and implementation of an interleaved three-level PWM DC/DC ZVS converter," *International Journal of Electronics*, vol. 103, pp. 322-341, 2016.
[21] R. Beiranvand, B. Rashidian, M. R. Zolghadri, and S. M. H. Alavi, "Designing an adjustable wide range regulated current source," *IEEE Transactions on Power Electronics*, vol. 25, pp. 197-208, 2010.
[22] R. Beiranvand, B. Rashidian, M. R. Zolghadri, and S. M. H. Alavi, "Using LLC resonant converter for designing wide-range voltage source," *IEEE Transactions on Industrial Electronics*, vol. 58, pp. 1746-1756, 2011.
[23] M. T. Outeiro, G. Buja, and D. Czarkowski, "Resonant Power Converters: An Overview with Multiple Elements in the Resonant Tank Network," *IEEE Industrial Electronics Magazine*, vol. 10, pp. 21-45, 2016.
[24] B. R. Lin and C. W. Chu, "A new parallel ZVS converter with less power switches and low current stress components," *International Journal of Circuit Theory and Applications*, 2015.
[25] B. R. Lin and C. W. Chu, "Hybrid DC–DC converter with high efficiency, wide ZVS range, and less output inductance," *International Journal of Circuit Theory and Applications*, 2015.
[26] B.-R. Lin and C.-H. Chao, "Soft-switching converter with two series half-bridge legs to reduce voltage stress of active switches," *IEEE Transactions on Industrial Electronics*, vol. 60, pp. 2214-2224, 2013.
[27] A. Polleri and M. Anwari, "Modeling and Simulation of Paralleled Series-Loaded-Resonant Converter," *in 2008 Second Asia International Conference on Modelling &# x00026; Simulation (AMS), pp. 974-979, 2008.*
[28] M. Salem, A. Jusoh, N. R. N. Idris, and I. Alhamrouni, "Steady state and generalized state space averaging analysis of the series resonant converter," in *Clean Energy and Technology (CEAT) 2014, 3rd IET International Conference on, pp. 1-5, 2014.*
[29] R. M. Schupbach and J. C. Balda, "Comparing DC-DC converters for power management in hybrid electric vehicles," *in Electric Machines and Drives Conference, 2003. IEMDC'03. IEEE International, pp. 1369-1374, 2003.*
[30] N. Mohan and T. M. Undeland, Power electronics: converters, applications, and design: John Wiley & Sons, 2007.

## BIOGRAPHIES OF AUTHORS

Mohamed Salem was born in Libya in 1984. He received his B.Eng. degree from Elmergib University, Al Khums, Libya, in 2007. The M.Sc. degree in electrical power electronics from Tun Hussein Onn University of Malaysia, Batu Pahat, Johor, Malaysia, in 2011. Currently, he is a candidate for Ph.D degree in Department of Power Engineering, Faculty of Electrical Engineering, Universiti Teknologi Malaysia, Malaysia. His research interests are in DC-DC converter, renewable energy applications, energy Conversion, and control of power electronics systems.

Awang Jusoh was born in Terengganu, Malaysia in 1964. He received his B.Eng. degree from Brighton Poly-technic, U.K., in 1988. He obtained his M.Sc. and Ph.D. degrees from the University of Birmingham, U.K., in 1995 and 2004, respectively. He is currently an associated Professor in the Department of Power Engineering, Faculty of Electrical Engineering, Universiti Teknologi Malaysia, Malaysia. His research interests are in DC-DC converter, renewable energy, and control of power electronics system.

Nik Rumzi Nik Idris (M'97–SM'03) received the B.Eng. degree in electrical engineering from the University of Wollongong, Wollongong, Australia, in 1989, the M.Sc. degree in power electronics from Bradford University, Bradford, U.K., in 1993, and the Ph.D. degree from the Universiti Teknologi Malaysia, Johor, Malaysia, in 2000. He was a Visiting Research Associate at the University of Akron, Akron, OH, in 2002. Currently, he is an Associate Professor at the Universiti Teknologi Malaysia. His research interests include AC drive systems and DSP applications in power electronic systems. He is a Senior Member of the IEEE Industry Applications, IEEE Industrial Electronics, and IEEE Power Electronics Societies.

Tole Sutikno is an Associated Professor in Department of Electrical Engineering at Universitas Ahmad Dahlan (UAD), Indonesia. He is Editor-in-Chief, Principle Contact and Editor for some Scopus indexed journals. He is also one of founder of the Indonesian Publication Index (IPI). He has completed his studies for B.Eng., M.Eng., Ph.D. in Electrical Engineering from Diponegoro University, Gadjah Mada University and Universiti Teknologi Malaysia, respectively. His research interests include the field of industrial electronics and informatics, power electronics, FPGA applications, embedded systems, data mining, information technology and digital library

Iftikhar Abid is a Senior Power Electronics Engineer in Advanced Photon Source, Argonne National Laboratory, USA. He has Graduated from MUET Sindh in 2007-8 as a B.E Electronics. He has been working in the field of Power Electronics since graduation.